EPJ AP

Applied Physics

EPJ .org
your physics journal

Eur. Phys. J. Appl. Phys. (2013) 62: 10202 DOI: 10.1051/epjap/2013120061

Structural characterization and electrical properties of nanostructured 4-tricyanovinyl-N,N-diethylaniline thin films

M.M. El-Nahass, H.M. Zeyada, K.F. Abd-El-Rahman, and Ahmed A.A. Darwish

The title “The European Physical Journal” is a joint property of EDP Sciences, Società Italiana di Fisica (SIF) and Springer

Eur. Phys. J. Appl. Phys. (2013) 62: 10202
DOI: 10.1051/epjap/2013120061

THE EUROPEAN PHYSICAL JOURNAL APPLIED PHYSICS

Regular Article

Structural characterization and electrical properties of nanostructured 4-tricyanovinyl-N,N-diethylaniline thin films

M.M. El-Nahass[1], H.M. Zeyada[2], K.F. Abd-El-Rahman[1], and Ahmed A.A. Darwish[1,3,a]

[1] Department of Physics, Faculty of Education, Ain Shams University, Rorxy Square, Cairo 11757, Egypt
[2] Department of Physics, Faculty of Science, Damietta University, New Damietta 34517, Egypt
[3] Department of Physics, Faculty of Education at Al-Mahweet, Sana'a University, Al-Mahweet, Yemen

Received: 15 February 2012 / Received in final form: 13 October 2012 / Accepted: 8 March 2013
Published online: 23 April 2013 – © EDP Sciences 2013

Abstract. X-ray diffraction (XRD) patterns indicated that the powder of 4-tricyanovinyl-N,N-diethylaniline (TCVA) has a polycrystalline structure with triclinic crystal system. The scanning electron microscope of the as deposited TCVA thin film shows a nanocrystalline structure with crystallite size of 45–75 nm. The crystallite size increases by increasing film thickness and annealing temperatures. The dark electrical resistivity decreases with increasing film thickness. Such variations are a consequence of crystallite size effect on the electrical resistivity of the films. The conductivity of the films measured in air is high in comparison to those measured under vacuum by one order. The removal of the hydroxyl group states by evacuation decreased the electrical conductivity of TCVA films. The temperature dependence of the electrical conductivity of TCVA films shows that the conduction is through a thermally activated process having two conduction mechanisms. The average values of activation energies are 0.28 and 0.74 eV for extrinsic and intrinsic conduction mechanisms, respectively. H-O group adsorption is responsible for the extrinsic conduction in TCVA films.

1 Introduction

Several features of organic materials make them attractive candidates in electronic and optoelectronic device applications. The actual fabrication of the organic-based devices can be considered as simple and economical techniques compared to the techniques currently used in most inorganic systems.

The search for new materials with good performance characteristics as well as the improvement in device fabrication has been also a subject of interest. Donor-acceptor (D-A) chromophores are considered as an important class of dyes having potential applications in different fields such as photographic sensitizer [1] and optoelectronics devices [2]. Moreover, there is a renewed interest in this kind of compounds because of their high dipole moments and strong intermolecular charge-transfer bands are at the origin of their first molecular hyperpolarizabilities and because of their second-order nonlinear optical response [3,4]. 4-tricyanovinyl-N,N-diethylaniline (TCVA) is disubstituted benzenes of the type donor-acceptor with an electron donor (diethylamino group) and an electron acceptor (tricyanovinyl group) [5,6], where its molecular structure is depicted in Figure 1. This dye belongs to a class of organic compounds known as molecular rotors [6–8], which have a great importance as fluorescence probes [9–13].

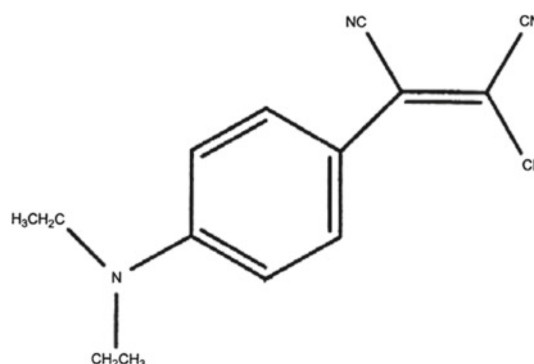

Fig. 1. Molecular structure of TCVA compound.

The electrical conductivity of organic compounds arises from delocalized π-electrons, the presence of functional groups, adsorbed species and defect sites [14]. Gas adsorption by organic compounds is an important issue for both fundamental research and technique applications of organic compounds. The electronic transport properties of organic compounds are sensitive to adsorption of selective gases [15–18]. Therefore, it is possible to construct sensors based on the organic compounds [18,19].

This research reports the structural properties of newly synthesized organic compound (TCVA) [20,21] in powder

[a] e-mail: aaadarwish@gmail.com

form and thin film conditions, as well as the effects of film thickness and annealing temperatures on its structural and electrical properties, moreover the influence of surface states and gas adsorption on its electrical conductivity has been investigated.

2 Experimental details

The TCVA compound was prepared by direct reaction between N,N-diethylaniline and tetracyanoethylene and the synthesis was described previously [20,21]. The differential scanning calorimeter results on TCVA compound showed that this compound is stable up to 423 K [22].

The glass substrates were used for depositing films for the X-ray diffraction and the electrical measurements, potassium bromide (KBr) single crystal substrates were used for depositing films for IR measurements and optically flat amorphous quartz substrates were used for depositing films for the optical measurements. Since the state of the substrate surface greatly affects the growth of the deposited film, the KBr substrates were firstly cleaved to be an optical flat surface. The glass and quartz substrates have been cleaned sequentially according to the following steps: immersion in chromic acid for 24 h; followed by washing several times with distilled water, rinsing by isopropyl alcohol, drying with dry air and finally they were cleaned by atomic bombardment in an initial stage of evacuation by a coating unit.

TCVA films were prepared by the thermal evaporation technique using a high vacuum coating unit (Edwards, E306A). Thin films were deposited from a titanium evaporator charged by TCVA in a vacuum of 10^{-4} Pa. The material was heated up by passing a suitable current through the titanium evaporator. The quartz crystal thickness monitor (Edwards, FTM4) controls the deposition rate (5 nm s^{-1}) and the thickness of the evaporated films. The interferometer method of thickness measurement [23] was also applied to check the thickness of the evaporated films.

The effects of the annealing temperatures on the structural properties of the TCVA thin films were performed. The heat treatment cycle consists of heating the samples in air up to 373 and 423 K with a soaking time of 2 h followed by furnace cooling down to the ambient temperature.

XRD patterns of TCVA in powder form, as deposited and annealed thin films were performed by XRD system (Philips X' pert MPD) equipped with Cu target. The Ni-filtered Cu K_α radiation ($k_{\alpha 1} = 0.15408$ nm) was used. The X-ray tube voltage and current were 40 kV and 30 mA, respectively. The diffractometer recorded the diffraction patterns automatically with a scanning speed of 2 degrees per minute. However, for determination of the crystallite size of the as deposited and annealed films the scanning speed for individual peaks was 0.5 degree per minute. The electron microscope (JEOL JSM-T200) examines the microstructure of the film.

Hot probe method [24,25] specified the type of the semiconductor and showed that TCVA is a p-type semiconductor. For the electrical measurements, the films were in the planar configuration of thicknesses ranging from 315 to 1020 nm. The Ohmic contacts were made by evaporating high purity Au through masks on the films at a vacuum of 10^{-4} Pa. The Ohmic contact was checked by I-V characteristics at room temperature. A high impedance electrometer (Keithley, Model 610) measures the electrical resistance of TCVA films by the two-probe method. The film resistance (R) was measured five times and its average value was determined. The film specific resistivity (ρ_f) has been calculated according to the following equation:

$$\rho_\mathrm{f} = R\frac{A}{L}, \tag{1}$$

where A stands for the cross-sectional area of the film and L refers to its length. The dark electrical conductivity (σ) is the reciprocal of ρ_f.

The temperature was measured by NiCr-NiAl thermocouple monitored by a micro-voltmeter. The dark electrical conductivity (σ) as a function of temperature in air as well as under vacuum of $\sim 10^{-1}$ Pa was monitored by using a two-probe technique powered by a stabilized dc power supply.

3 Results and discussion

3.1 Structural characterizations

XRD patterns of TCVA in the powder form were undertaken at room temperature (298 K) in 2θ range from 5 to 60°. Figure 2 presents the XRD patterns for the powder of TCVA compound; it shows that the powder of TCVA is polycrystalline. The CRYSFIRE computer program [26] indexes all the diffraction lines and calculates the lattice parameters. The analysis indicated that TCVA has triclinic crystal system with space group $P\bar{1}$ and the lattice parameters are given as $a = 0.765$ nm, $b = 0.778$ nm, $c = 1.367$ nm, $\alpha = 104.42°$, $\beta = 95.63°$ and $\gamma = 105.36°$. CHECKCELL program [27] calculates the indicated Miller indices (hkl) on each diffraction peak. For the sample in powder form, a major peak is observed at about ($2\theta = 21.32°$) and its interplanar spacing is 0.698 nm, which corresponds to reflection from $(0\,\bar{1}\,1)$ plane of triclinic crystal system.

Figure 3 shows a micrograph of the as deposited TCVA thin film of thickness 1020 nm. The obtained structure has a crystallite size in the range of 60–70 nm indicating that the as deposited TCVA thin film has a nanocrystallite structure. The obtained microstructure can be attributed to the triclinic system crystallographic symmetry and to the preferred orientation formed during the deposition process of TCVA films.

Figure 4 illustrates XRD patterns of the as deposited TCVA thin film with different thicknesses ranging from 315 to 1020 nm. In the case of TCVA film of thicknesses 315 nm, there is only one significant peak at $2\theta = 7.25°$ corresponding to the reflection plane of (0 0 1) and this implies that a polycrystalline structure of powder TCVA became nanocrystallite structure in the film form. Increasing

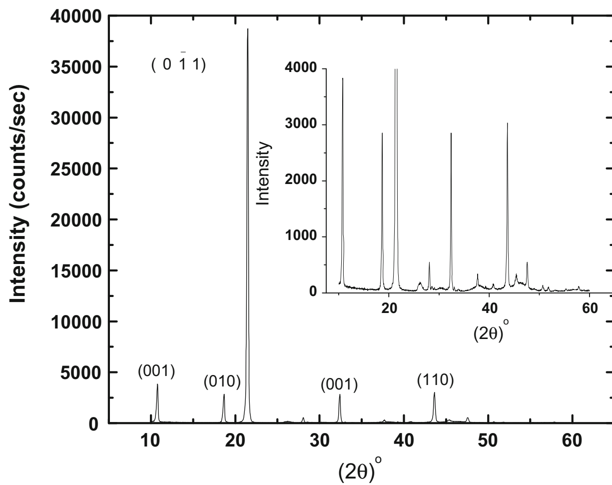

Fig. 2. X-ray diffraction pattern of TCVA compound in the powder form.

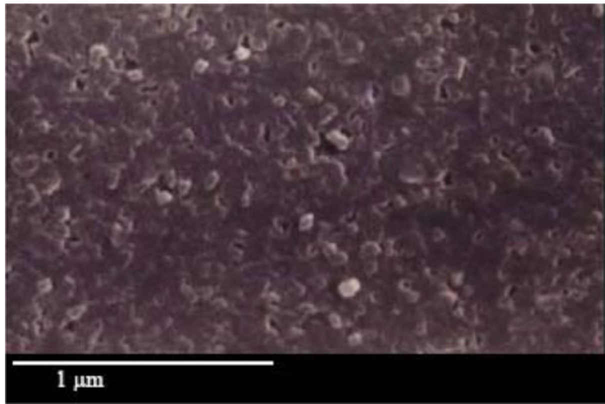

Fig. 3. SEM micrograph for as deposited TCVA thin film of 1020 nm thicknesses.

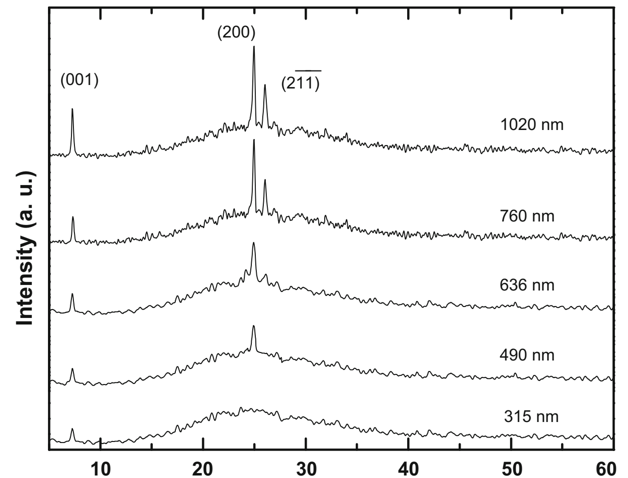

Fig. 4. X-ray diffraction patterns for as deposited TCVA films of different thicknesses.

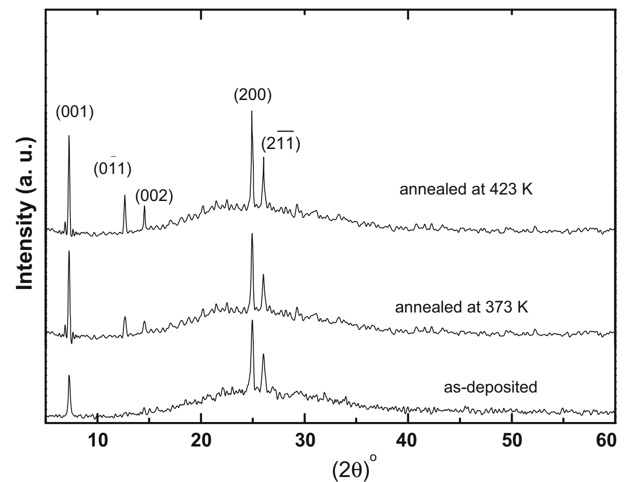

Fig. 5. X-ray diffraction patterns for as deposited and annealed TCVA films. Film thickness is 1020 nm.

film thickness did not affect the position of the (0 0 1) diffraction peak. However, new additional diffraction peaks appear and the integrated intensity of those diffraction peaks increases with the increase in the film thickness indicating that increasing the film thickness increased the nanocrystallite size of the as deposited TCVA thin films.

In order to investigate the effect of the annealing temperatures on the structure of the TCVA films, annealing in air at 373 and 423 K with soaking time of 2 h was performed for the film with a thickness of 1020 nm. Figure 5 presents XRD patterns of the as deposited and annealed TCVA films. Increasing the annealing temperature increases both the number and the integrated intensities of diffraction peaks in TCVA films, this indicates that the crystallite size of the formed nanocrystallite structure increases by annealing.

It is well known that the shape of each X-ray diffraction peak results from the combined effects of the crystallite size, internal strain (microstrain), point defects and instrumental broadening. Assuming that the influence of point defects is weak in this case, the crystallite size, D, can be calculated according to the Scherrer formula [28,29] as:

$$D = \frac{K_S \lambda}{\beta \cos\theta}, \tag{2}$$

where λ is the X-ray wavelength of Cu K_α (0.15418 nm), θ is the corresponding Bragg diffraction angle and K_S is the Scherrer's constant, which is in order of unity (~ 0.95) [29]. In addition, β is obtained from the measured peak with β_m in the diffraction pattern [29] (β_m is the full-width at half maximum (FWHM), of the diffraction peak in radians) and is given by:

$$\beta^2 = \beta_m^2 - \beta_{inst}^2. \tag{3}$$

The instrumental broadening β_{inst} was determined by measurements on annealed TCVA powder material. The dislocation density (δ) is the number of dislocation lines per unit area of the film. The following formula determines δ [30]:

$$\delta = \frac{1}{D^2}. \tag{4}$$

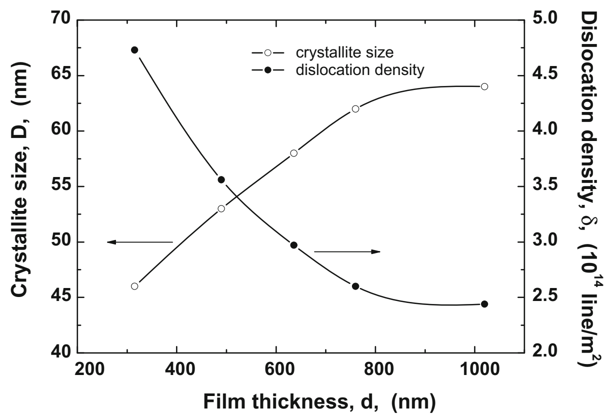

Fig. 6. The mean crystallite size, D, and dislocation density, δ, as a function of the film thickness, d.

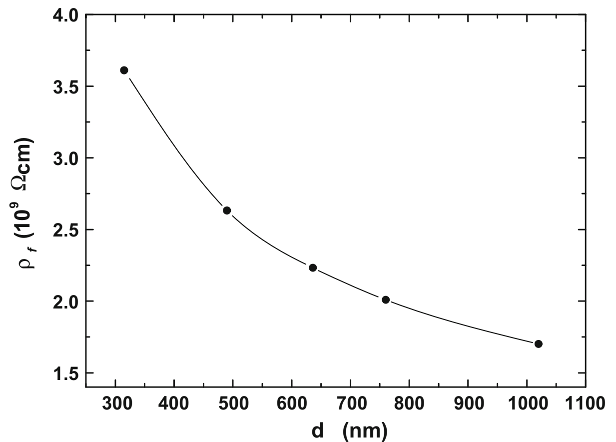

Fig. 7. Dependence of the dark resistivity on the film thickness for TCVA films at room temperature.

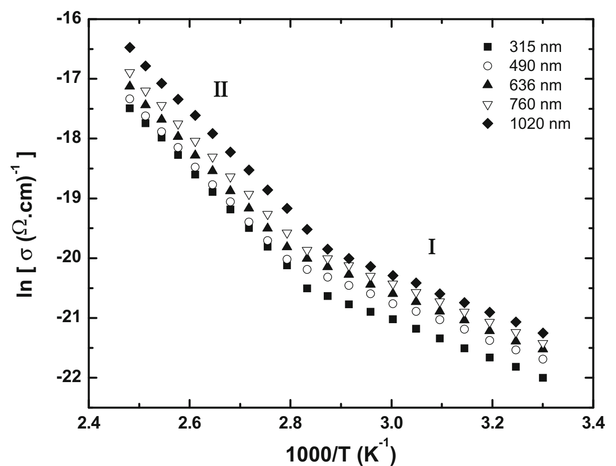

Fig. 8. Temperature dependence of the electrical conductivity of TCVA thin films with different thicknesses.

Figure 6 illustrates the variation of the crystallite size and the dislocation density with film thickness for the as deposited TCVA films. It can be observed that the dislocation density decreases and the crystallite size of the formed nanocrystallite increases with increasing film thickness and they reached a constant value at 1020 nm film thickness. Increasing film thickness reduces the dislocation density and this is due to the release of internal stresses in the films. The crystallite size increases nonlinearly with the increase of film thickness and it arrives to a constant value for higher thicknesses. It is also clear that the crystallite size is in the nanoscale range and it varies from 45 nm to 65 nm depending on the thickness; such a result well agreed with the previously obtained one by SEM. The gradual reduction in the stacking fault of the layers with an increase in the film thickness may be responsible for the reduction in the dislocation density [31]. However, it is observed that the nanocrystallite size increases and dislocation density decreases with increasing annealing temperatures. The crystallite size of TCVA films increases from 64 to 169 nm upon increasing annealing temperatures to 423 K. The decrease in full-width at half maximum and dislocation density with increasing annealing temperatures is a result of refinement of nanocrystallite size and annihilation of dislocations by annealing.

3.2 Electrical measurements

Figure 7 shows the dark electrical resistivity (ρ_f) of TCVA films versus film thickness. The measurements were performed at room temperature for different thicknesses ranging from 315 to 1020 nm. As illustrated, the dark electrical resistivity decreases nonlinearly with increasing film thickness. Such a decrease is well discussed in terms of the film growth mechanism where as the film thickness increases, the crystallite size and mobility of charge carriers increase and hence the resistivity of the film decreases. Such a decrease in resistivity continues up to reaching a relatively thick film at which the structure of the film resembles that one of the bulk material.

The temperature dependence of the electrical conductivity for TCVA thin films was studied in the temperature range from 298 to 403 K. Figure 8 illustrates the variation of the electrical conductivity as a function of temperature for TCVA films with different film thicknesses. The results show that the TCVA films behave as a semiconductor material. The increase of the conductivity with increasing film thickness and annealing temperature is attributed to the increase of the crystallite size with increasing film thickness and annealing temperatures as previously shown in Figures 5 and 6. Figure 8 indicates that the conduction is through a thermally activated process having two conduction mechanisms. The straight lines, identified as (I) and (II), indicated the validity of a two component Arrhenius equation [32] where:

$$\sigma = \sigma_{o1} \exp(-\Delta E_1/k_B T) + \sigma_{o2} \exp(-\Delta E_2/k_B T), \quad (5)$$

where σ_{o1} and σ_{o2} are the pre-exponential factors, ΔE_1 and ΔE_2 are the electrical activation energies in regions (I) and (II) respectively and k_B is the Boltzmann constant. The values of the activation energies for both regions can be obtained from the slopes of the lines however the values

Table 1. Values of the pre-exponential factors versus film thickness for TCVA compound.

Film thickness nm	$\sigma_{o1} \times 10^{-5}$ Ω^{-1} cm^{-1}	σ_{o2} Ω^{-1} cm^{-1}
315	1.10	42.93
490	1.52	60.15
636	2.04	63.95
760	2.59	77.58
1020	2.91	115.16

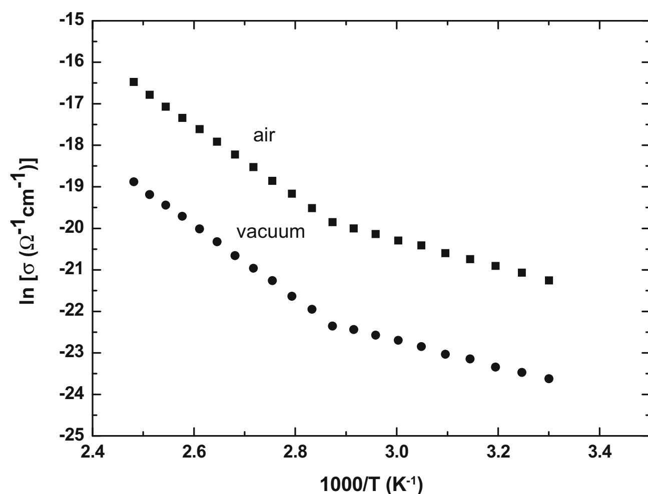

Fig. 9. The relation between ln σ and $1000/T$ for TCVA films at air and under vacuum conditions.

of conductivity pre-exponential factors can be estimated from the intercept of lines with the ordinate axis. The values of activation energies and pre-exponential factors are listed in Table 1. It has been found that the values of the pre-exponential factors are thickness dependent. Also the values of activation energies for the two regions were found to be $\Delta E_1 = 0.28$ eV and $\Delta E_2 = 0.74$ eV, respectively. This leads us to suggest that there are two different conduction mechanisms for the two regions, intrinsic and extrinsic, which are in good agreement with the results obtained by [33,34]. The obtained slopes of the curves in the two regions were found to be independent of the film thickness; this indicates that the activation energies are independent of the film thickness in the thickness range of 315–1020 nm.

Figure 9 depicts the dark electrical conductivity, σ, as a function of temperature for TCVA film with thickness 1020 nm at two environmental conditions (in air and under vacuum). The conductivity of the films measured in air is high in comparison to those measured under vacuum by one order. This behavior is a result of an increase in the majority carrier concentrations resulting from oxygen adsorption [35]. Similar observations have been reported on some other organic compounds such as lead phthalocyanine, PbPc [35], CuPc [36] and CoPc [37] films.

The electrical properties of thin semiconductor films strongly depend on their structure and purity [35].

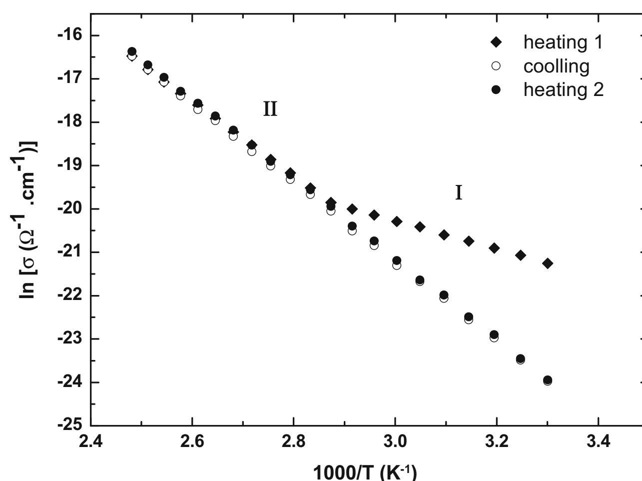

Fig. 10. Temperature dependence of the electrical conductivity of TCVA thin film: ◇ – 1st heating run, o – cooling run and • – 2nd heating run.

Heating of the film may modify these characteristics and consequently, the electrical properties of the respective film (particularly, electrical conduction) may vary too. The study of the electrical conductivity during isochronal annealing may provide information on the processes taking place in the respective films. In this connection, the shape of the ln σ versus $10^3/T$ curves during this treatment was examined. Figure 10 demonstrates the DC conductivity results for TCVA film with thickness 1020 nm. The curve with dark rhombus in the figure shows the results of DC conductivity for temperatures increasing up to 400 K, followed by the results of the curve with open circle of ln (σ) versus $10^3/T$ obtained with temperatures decreasing from 400 K down to room temperature. The curve with dark circles indicates the ln (σ) versus $10^3/T$ characteristics of the last heating cycle to 400 K which is also shown in Figure 10. It is clear from the characteristics shown in Figure 9 that the first heating run consists of two different temperature regions with two different activation energies. The temperature region (I) is in the temperature range 300–353 K and the temperature region (II) is for temperatures greater than 353 K. The calculated activation energies for regions (I) and (II) are 0.28 and 0.74 eV, respectively. The value of activation energy in the temperature region (II) is almost half the value of the optically estimated energy gap (1.45 eV) of the TCVA films [21]. Therefore, we can suggest that the first region is due to extrinsic behavior and the second one is due to intrinsic behavior. The pioneer's work [33,34] supports this suggestion. FTIR measurements of the as deposited TCVA films indicate the presence of O-H band at 3433 cm^{-1} and they also demonstrate the absence of O-H band for annealed TCVA films [21]. The presence of the hydroxyl group (O-H band) in the IR spectrum of the as deposited TCVA film indicates that the material adsorbs hydroxyl group from ambient atmosphere. The adsorbed species act as an acceptor impurity that increases the electrical conductivity (extrinsic region of conduction). This is in good

agreement with the results obtained by Twarwoski [39] who studied the effect of oxygen doping in ZnPc films and suggested that oxygen molecules diffuse into the films, hence acting as an electron-acceptor dopant that creates p-type charge carriers in the Pc and makes the current increase. This is quite clear during the first heating run where an activation energy corresponding to the extrinsic conduction occurs. When the temperature reaches 343 K, hydroxyl group leaves the TCVA compound, therefore TCVA compound acts as an intrinsic semiconductor. For clarifying this idea, the ln (σ) versus $1000/T$ characteristics of the sample were measured during the cooling and the second heating runs. Figure 10 shows that there is one temperature region in both cooling and second heating runs that extends from room temperature up to 410 K. The calculated activation energy in this temperature region is equal to that one for intrinsic region of conduction.

4 Summary and conclusions

X-ray diffraction patterns of powder TCVA compound indicate that the material is polycrystalline with triclinic crystal system. The thermally evaporated TCVA thin films have a nanocrystallite structure with crystallite size in the range of 45–75 nm. The crystallite size increases with increasing film thickness and annealing temperatures. The dark electrical resistivity decreases with increasing film thickness. The temperature dependence of the electrical conductivity in TCVA films indicates that the conduction is through a thermally activated process having two conduction mechanisms. The calculated values for pre-exponential factors and activation energies suggest that the electrical conduction takes place by an extrinsic conduction in the temperature range from room temperature up to 353 K and it is by an intrinsic conduction mechanism for temperatures greater than 353 K. The adsorption of H-O group by TCVA film is responsible for its extrinsic conduction. Further work on TCVA film is needed in future to apply this compound as a sensor.

References

1. H. Rlngsdorf, L. Cabres, A. Dittrich, Ang. Chem. Int. Ed. **30**, 76 (1991)
2. D.J. Willhams, Ang. Chem. Int. Ed. **23**, 690 (1984)
3. H.S. Miyata, *Nonlinear Optics of Organic Molecules and Polymers* (CRC Press, Boca Raton, 1997)
4. J.J. Wolf, R. Wortmann, Adv. Phys. Org. Chem. **32**, 12 (1999)
5. A. Safarzadeh-Amiri, Can. J. Chem. **62**, 1895 (1984)
6. R.O. Loutfy, K.Y. Law, J. Phys. Chem. **84**, 2803 (1980)
7. R.O. Loutfy, Pure Appl. Chem. **58**, 1239 (1986)
8. M.S.A. Abdel-Mottaleb, R.O. Loutfy, R. Lapouyade, J. Photochem. Photobiol. A **48**, 87 (1989)
9. R.O. Loutfy, K.Y. Law, Macromolecules **14**, 587 (1981)
10. K.Y. Law, Chem. Phys. Lett. **75**, 545 (1980)
11. K.Y. Law, Photochem. Photobiol. **33**, 799 (1981)
12. R.O. Loutfy, B.A. Arnold, J. Phys. Chem. **86**, 4205 (1982)
13. R.O. Loutfy, Macromolecules **16**, 678 (1983)
14. P.G. Collins, K. Bradley, M. Ishigami, A. Zettl, Science **287**, 1801 (2000)
15. A.M. Saleh, R.D. Gould, A.K. Hassan, Phys. Status Solidi. A **139**, 334 (1993)
16. R.A. Collins, K.A. Mohammed, Thin Solid Films **145**, 133 (1986)
17. M. Sakaguchi, M. Ohta, J. Solid State Chem. **61**, 130 (1986)
18. B. Schollhorn, J.P. Germain, A. Pauly, C. Maleysson, J.P. Blanc, Thin Solid Films **326**, 245 (1986)
19. J.P. Germain, A. Pauly, C. Maleysson, J.P. Blanc, B. Schollhorn, Thin Solid Films **333**, 235 (1998)
20. A.M. Asiri, J. Saudi Chem. Soc. **6**, 51 (2002)
21. M.M. El-Nahass, H.M. Zeyada, K.F. Abd El-Rahman, A.A.M. Farag, A.A.A. Darwish, Spectrochimica Acta Part A **69**, 205 (2008)
22. M.M. El-Nahass, K.F. Abd-El-Rahman, A.A.A. Darwish, Physica B **403**, 219 (2008)
23. S. Tolansky, *Multiple – Beam Interference Microscopy of Metals* (Academic Press, London, 1970)
24. D.K. Schroder, *Semiconductor Material and Device Characterization* (John Wiley & Sons, Inc., New York, 1998)
25. Keithley Instruments, Inc., *Low Level Measurements Handbook*, 6th edn. (Keithley Instruments, Inc., Cleveland, Ohio, 2004)
26. R. Shirley, *The CRYSFIRE System for Automatic Powder Indexing: User's Manual* (The Lattice Press, Guildford, England, 2000)
27. J. Laugier, B. Bochu, *LMGP-Suite suite of Programs for the Interpretation of X-ray Experiments, ENSP/Laboratoire des Matériaux et du Génie Physique* (Saint-Martin-d'Hères, France, 2000)
28. V. Holý, U. Pietsch, T. Baumbach, *High Resolution X-ray Scttering From Thin Films and Multilayers* (Springer, Berlin, 1999)
29. A.K. Hassan, R.D. Gould, Phys. Status Solidi A **132**, 91 (1992)
30. S. Velumani, X. Mathew, P.J. Sebastian, Solar Energy Mater. Solar Cells **76**, 359 (2003)
31. T. Mahalingam, S. Thanikaikarasan, R. Chandramohan, M. Raja, C. Sanjeeviraja, J.-H. Kim, Y.D. Kim, J. Mater. Chem. Phys. **106**, 369 (2007)
32. B.A. El-Sayed, M.M. Sallam, M.F. Ishak, M.S. Antonious, Mater. Lett. **34**, 280 (1998)
33. E. Gutmann, L.E. Lyons, *Organic Semiconductors Part A* (Robert E. Krieger Publishing Co., 1981)
34. M. Pope, C.E. Swenberg, *Electronic Processes in Organic Crystals and Polymers*, 2nd edn. (Oxford University Press, Oxford, 1999)
35. T.S. Shafai, R.D. Gould, Thin Solid Films **516**, 383 (2007)
36. R.D. Gould, A.K. Hassan, Thin Solid Films **516**, 334 (2007)
37. S.I. Shihub, R.D. Gould, S.G. Navano, Physica B **222**, 136 (1966)
38. V. Şunel, G.I. Rusu, G.G. Rusu, L. Leontie, C. Şoldea, Prog. Org. Coatings **26**, 53 (1995)
39. A. Twarwoski, J. Chem. Phys. **77**, 5840 (1983)